Rev. Letters 26, 1416 (1971).

[6]L. V. Keldysh, Zh. Eksperim. i Teor. Fiz. 47, 1945 (1964) [Sov. Phys. JETP 20, 1307 (1965)].

[7]H. B. Bebb and A. Gold, Phys. Rev. 143, 1 (1966).

[8]V. M. Morton, Proc. Phys. Soc. (London) 92, 301 (1967).

[9]F. T. Chan and C. L. Tang, Phys. Rev. 185, 42 (1969).

[10]Y. Gontier and M. Trahin, Phys. Rev. A 4, 1896 (1971).

[11]B. A. Zon, N. L. Manakov, and L. P. Rapoport, Zh. Eksperim. i Teor. Fiz. 61, 968 (1971) [Sov. Phys. JETP 34, 515 (1972)].

[12]S. L. Chin, Phys. Rev. A 4, 992 (1971).

[13]N. K. Berejetskaya, G. S. Voronov, G. A. Delone, N. B. Delone, and G. K. Piskova, Zh. Eksperim. i Teor. Fiz. 58, 753 (1970) [Sov. Phys. JETP 31, 403 (1970)].

[14]F. V. Bunkin, R. V. Karapetyan, and A. M. Prokhorov, Zh. Eksperim. i Teor. Fiz. 47, 216 (1964) [Sov. Phys. JETP 20, 145 (1965)].

[15]F. V. Bunkin and I. I. Tugov, Zh. Eksperim. i Teor. Fiz. 58, 1987 (1970) [Sov. Phys. JETP 31, 1071 (1970)].

[16]T. E. Sharp, Atomic Data 2, 119 (1971).

[17]G. Herzberg, *Spectra of Diatomic Molecules* (Van Nostrand, New York, 1950).

[18]The band origin corresponding to the $X\,^1\Sigma_g(v=0) \rightarrow E, F\,^1\Sigma_g(v=21)$ six-photon transition was obtained by adding the term value $T_0 = 90\,204$ cm^{-1} of the B state, the energy of the $0 \rightarrow 0$ band of the $E, F \rightarrow B$ transition (8961 cm^{-1}) and the energy difference between the $v=21$ and $v=0$ levels of the E, F state. This last term was calculated by W. Kolos and L. Wolniewicz [J. Chem. Phys. 50, 3228 (1969)]. The resonance gap lies close to the bandwidth of the laser radiation.

[19]The total energy of the transitions corresponding to a given band of the Lyman $X \rightarrow B$ system was calculated using Dunham nomenclature. The spectroscopic constants for the X and B states of H_2 were taken from B. Rosen [*International Tables of Selected Constants: Spectroscopic Data Relative to Diatomic Molecules* (Pergamon, New York, 1970), Vol. 17.]

[20]The rotational structure of the $0 \rightarrow 3$ band of the $X \rightarrow B$ system of H_2 is much more open than that of E, F ($v=21$) level. Successive rotational lines for $k=5$ are separated by about 150 cm^{-1}, which is the condition for resonance. Multiphoton absorption may be only satisfied by the single rotational $B\ ^1\Sigma_u$ ($v=3$, $k=5$) level achievable through five-photon absorption for which the resonance gap lies close to the bandwidth of the laser radiation.

[21]R. S. Berry and S. E. Nielsen, Phys. Rev. A 1, 395 (1970).

[22]F. V. Bunkin and I. I. Tugov, Phys. Rev. (to be published).

[23]G. H. Dunn, Phys. Rev. 172, 1 (1968); and also, Yu. D. Oksyuk, Opt. i Spektroskopiya 23, 213 (1967) [Opt. Spectry. (USSR) 23, 115 (1967)].

[24]J. L. Debethune, Nuovo Cimento (to be published).

[25]B. Held, G. Mainfray, and J. Morellec, Phys. Letters 39A, 57 (1972).

[26]H. R. Reiss, Phys. Rev. D 4, 3533 (1971).

PHYSICAL REVIEW A VOLUME 7, NUMBER 1 JANUARY 1973

Determination of the H-He Potential from Molecular-Beam Experiments

R. Gengenbach, Ch. Hahn, and J. P. Toennies
Physikalisches Institut der Universität, Bonn
and Max-Planck-Institut für Strömungsforschung, Göttingen, Germany
(Received 24 April 1972)

Absolute total cross sections for D-He scattering were measured with an accuracy of 1% at 0.3, 0.5, and 0.6 eV. These new data were combined with published relative measurements of the velocity dependence of the H-He cross section in a χ^2 minimalization procedure. The resulting potential $V(R)$ as function of internuclear separation R is precisely determined in the repulsive range $1.7\ \text{Å} < R < R_0$ with $V(R_0) = 0$. Several multiparameter potential models were tried. Of these the four-parameter *ansatz* $V(R) = A(e^{-\alpha R} - e^{-\alpha R_0})$ (for $R < R_0$) $= 4\epsilon[(R_0/R)^{12} - (R_0/R)^6]$ (for $R > R_0$) was found to describe the data best. Parameters obtained are $A = 70.00$ eV, $\alpha = 3.383$ Å^{-1}, $R_0 = 3.20$ Å, and $\epsilon = 0.39$ meV. The well depth ϵ, to which the measurements are insensitive, is chosen to match the theoretical van der Waals constant $C_6 = 2.83$ a.u. The potential is compared with results of *ab initio* calculations, and a probable ϵ range is discussed. For $0.35 \lesssim \epsilon \lesssim 0.70$ meV the calculated low-energy cross section shows a pronounced Ramsauer-Townsend minimum. The possibility of its observation is pointed out.

The H-He system is the simplest three-electron diatom and has been the object of numerous quantum-chemical *ab initio* calculations,[1-6] some of which have been performed over the entire (i.e., short, intermediate, and long) range of internuclear separations.[1,3,4,6] The most recent calculations show van der Waals wells,[3-6] the depth (ϵ) of which differs within an order of magnitude.

The H-He system is also of astrophysical interest. For instance, the infrared line shape in translational absorption is determined by the potential curve and has been suggested as being a possible factor in the opacity of late-type stars.[7] Furthermore, the potential is also needed to interpret hyperfine pressure-shift measurements on H in a He buffer gas.[3,6]

In order to get direct experimental information on the intermediate range of the potential, we have

precisely measured the absolute value of the total collision cross section in the scattering of D atoms[8] on He target gas at center-of-mass energies of 0.3, 0.5, and 0.6 eV.

The apparatus is essentially the same as described previously[9] (except for the target). An atomic deuterium beam is produced by thermal dissociation in a tungsten oven (exit slit 0.4×5 mm^2) heated by electron bombardment to 3000 °K. The target is a liquid-nitrogen cooled cylinder of 17 cm length and 15 cm diam, located 35 cm from the oven in a separately pumped chamber. The holes for beam entrance and exit are designed so that their conductance L can be calculated with an error of ±0.5%. The target is supplied with a constant flow $\dot{Q}$ of gas, which is measured to within ±0.5%,[10] so that the number density of target particles, $n=\dot{Q}/L$, can be determined to within 1%. A collimating slit of 2×5 mm^2 located 65 cm from the oven separates the target vessel from a third chamber, containing the standard mechanical velocity selector [velocity resolution $\Delta v/v=25\%$ full width at half-maximum (FWHM)]. From here the beam enters the electron-bombardment-mass spectrometer detector (background pressure 5×10^{-11} Torr) through a 2×5-mm^2 slit 140 cm from the oven. The ion pulses were counted by scalers with typical counting rates of 2500 per sec for the background, 1200 per sec for the unattenuated beam, and 600 per sec for the attenuated beam. Data reduction was done on line with a PDP 8/L computer.

Since the energy dependence of the total cross section of H-He in arbitrary units is known from other experiments,[11,12] we could restrict the absolute determination of the cross section to three primary beam velocities. The results are shown in Table I. The accuracy of the method was tested by measuring the cross section for He-He, where the potential is well known from molecular-beam experiments, measurements of bulk properties, and *ab initio* calculations. Our He-He cross sections are consistent with other values,[13] indicating that the systematic errors do not exceed 1%.

To determine the intermolecular potential the relative cross sections from Refs. 11 and 12 were combined with our absolute values in a χ^2 minimizing procedure. The criterion for the best potential $V_k=V_k(R;[A_k])$, where $[A_k]$ is a set of parameters which fits the three groups of data [$j=1$ (these data), $j=2$ (Ref. 11), $j=3$ (Ref. 12)], is that

$$\chi^2_{\mathrm{tot},k}=\sum_{j=1}^{3}\chi^2_{jk}(p_{jk},q_j,[A_k]) \qquad (1)$$

be minimal. The individual χ^2_{jk} measure the closeness of a fit, in which the trial potential V_k is used to interpret data from experiment j. They come from N_j measured cross sections $\hat{\sigma}_j(v_i)$ at velocities v_i with standard errors $\Delta\hat{\sigma}_j(v_i)$ and are given by

$$\chi^2_{jk}=\sum_{i=1}^{N_j}\left(\frac{(\bar{\sigma}_{jk}(v_i;[A_k])-p_{jk}\hat{\sigma}_j(v_i))}{p_{jk}q_j\,\Delta\hat{\sigma}_j(v_i)}\right)^2, \qquad (2)$$

where the two factors p_{jk} and q_j have been introduced to make a meaningful combination of the experimental data from the different sources possible. p_{jk} is a scaling factor for the measured $\hat{\sigma}_j$ and $\Delta\hat{\sigma}_j$ and q_j is an error-normalizing factor.[14] For the relative measurements p_{jk} ($j=2,3$) is chosen to minimize χ^2_{jk} for each set of $[A_k]$ without restrictions. For absolute measurements without systematic errors p_{1k} should be equal to 1. Due to the small systematic uncertainties of our experiment it is restricted to a 1% interval centered about unity. q_j is chosen from statistical considerations, which require that for a χ^2 distribution the minimum χ^2 should be equal to its expectation value df, i.e., the number of degrees of freedom.

In Eq. (2) the effective cross section $\bar{\sigma}_{jk}(v;[A_k])$ is calculated by standard techniques[13] as a function of primary beam velocity for the potential V_k and the experimental setup under study: First, scattering phase shifts $\eta_l(E_{\mathrm{c.m.}})$ are computed by Numerov integration of the radial Schrödinger equation at low energies and by the Jeffreys–Wentzel–Kramers–Brillouin–Langer (JWKBL) method (including Rosen and Yennie's correction term) at high energies $E_{\mathrm{c.m.}}$. From these η_l one obtains the partial cross sections $\sigma_l(E_{\mathrm{c.m.}})$, the total cross section $\sigma(E_{\mathrm{c.m.}})$, and the differential cross section $d\sigma(E_{\mathrm{c.m.}})/d\omega$. In order to correct $\sigma(E_{\mathrm{c.m.}})$ for the finite angular resolving power of apparatus j, $d\sigma/d\omega$ is folded with the angular-dependent detection probability $W_j(\theta)$ calculated by a Monte Carlo technique over all possible beam trajectories in the experimental setup j. After subtraction of the result from $\sigma(E_{\mathrm{c.m.}})$, this corrected cross section is finally averaged over the velocity distribution functions of primary beam and target gas. The accuracy of $\bar{\sigma}$ obtained in this

TABLE I. Measured effective cross sections $\hat{\sigma}$ for D-He at three primary beam velocities v, corresponding to center-of-mass energies $E_{\mathrm{c.m.}}$, with statistical standard errors $\Delta\hat{\sigma}/\hat{\sigma}$ of the mean, based on N single measurements. $\hat{\sigma}^*$ is the value of $\hat{\sigma}$ corrected for the experimental conditions of 77 °K target and 2800 °K oven temperature, 25% velocity resolution (FWHM), and the angular resolving power of the apparatus. $\hat{\sigma}^*$ can be compared with calculations of $\sigma(E_{\mathrm{c.m.}})$ without any further averaging.

v (m/sec)	$E_{\mathrm{c.m.}}$ (meV)	$\hat{\sigma}$ (Å^2)	$\hat{\sigma}^*$(Å^2)	$\Delta\hat{\sigma}/\sigma$(%)	N
7100	350.13	37.18	38.24	0.26	19
8390	488.90	35.97	37.25	0.47	30
9460	621.56	35.30	36.74	0.53	34

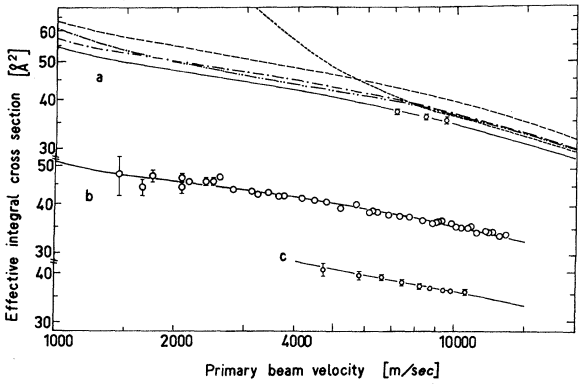

FIG. 1. (a) Measured absolute effective cross section $\hat{\sigma}_1$ for D-He taken at 77 °K target temperature as function of primary beam velocity, and calculated $\bar{\sigma}_{1k}$ for various potentials: broken line, Ref. 1; dash-dots, Ref. 3; dashed line, Ref. 4; dash–double-dot–dash, Ref. 6; solid line, this work. (b) Measured $\hat{\sigma}_3$ for H-He, taken from Ref. 12 (secondary beam at 77 °K, $\Delta v/v = 11\%$ FWHM), compared with $\bar{\sigma}_{3k}$, for best-fit potential (solid line). Error bars have been partly omitted. (c) Measured $\hat{\sigma}_2$ for H-He, taken from Ref. 11 (target at room temperature, $\Delta v/v = 25\%$ FWHM), compared with $\bar{\sigma}_{2k}$, for best-fit potential (solid line).

way is better than 0.3%.

Initially, potentials from the literature which covered a suitable range were evaluated as outlined above. The potential from Ref. 1 could be used in its analytical Slater–Buckingham form $V(R) = Ae^{-\alpha R} - C_6R^{-6}$, whereas the others, given in tabular form $[r_s, V(r_s)]$, $s = 1, 2 \cdots n$, had to be brought into a functional form in the interval $r_1 < R < r_n$ prior to calculation of $\bar{\sigma}$. We found cubic spline interpolation most suitable, and extended the spline, where no *ab initio* points were available, as

$$\begin{aligned} V(R) &= Ae^{-\alpha R} - A_0 && \text{for } R \le r_1 \\ &= \sum_{m=1}^{4} a_{1m}(R - r_1)^{m-1}, && r_1 < R \le r_2 \\ &= \sum_{m=1}^{4} a_{tm}(R - r_t)^{m-1}, && r_t < R \le r_n, \ t = n - 1 \\ &= -C_6R^{-6} - C_8R^{-8}, && r_n < R \,. \end{aligned} \tag{3}$$

Figure 1(a) shows the measured absolute cross sections $\hat{\sigma}_1$ and the calculated $\bar{\sigma}_{1k}$ for the potentials V_k listed in Table II, which contains the input parameters $[A_k]$ (upper part) and the resulting χ^2_{jk}, p_{1k}, and $\chi^2_{\text{tot},k}$ for the various experiments (lower part). Figures 1(c) and 1(b) show the measured

TABLE II. Comparison of potential parameters and χ^2 values.

		Potential parameters for H-He and D-He						This work, well from Eq. (4)
Ref.		1	3	4	6	5	6	
A (eV)		125.33	43.37	37.49	96.36	70.00	70.00	70.00
A_0 (meV)						1.39	1.39	1.39
α (Å^{-1})		3.326	2.940	2.865	3.360	3.383	3.383	3.383
n			10	10	16	7	11	
r_1 (Å)			1.06	1.06	1.59	3.17	3.17	
r_n (Å)			5.29	5.29	6.35	6.35	6.35	
R_0 (Å)		3.59	3.49	2.86	3.14	3.26	3.16	3.20
R_m (Å)		4.05	3.82	3.47	3.60	3.72	3.60	3.59
ϵ (meV)		0.22	0.30	3.24	0.96	0.46	0.96	0.39
C_6 (a.u.)		2.94	2.80	42.9	5.48	2.83	5.48	2.83
C_8 (a.u.)						41.9		
		Corresponding χ^2 for the experimental data from references						
this work	p_{1k}	1.010	1.010	1.010	1.010	1.000	0.995	1.000
	χ^2_{1k}	1386.0	244.2	922	124.2	3.0	3.2	3.5
11	χ^2_{2k}	8.2	8.0	763	9.4	10.7	9.7	10.6
12	χ^2_{3k}	46.0	51.0	17244	61.2	52.2	49.9	54.1
$\chi^2_{\text{tot},k}$ (df = 57)		1440.2	303.2	18929	194.8	65.9	62.8	68.2

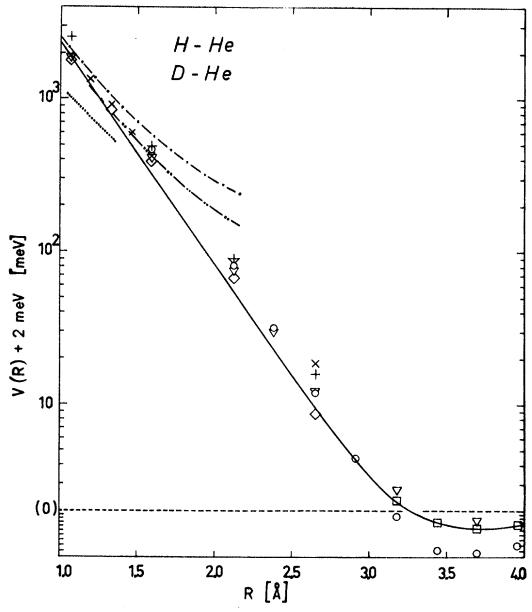

FIG. 2. Comparison of best-fit H-He, D-He potential, solid line (column 6, Table II) with results of *ab initio* calculations and experimental results at high energies: +, Ref. 1; ×, Ref. 2; ▽, Ref. 3; ◇, Ref. 4; □, Ref. 5; ○, Ref. 6; dash-dot-dash, Ref. 5 (wide detector); dash-dot-dot-dash, Ref. 5 (narrow detector); dots, Ref. 16.

relative cross sections $\hat{\sigma}_2$ and $\hat{\sigma}_3$ from Refs. 11 and 12, respectively. They have been shifted by factors $p_{2k'}$ and $p_{3k'}$ to give minimal $\chi^2_{2k'}$ and $\chi^2_{3k'}$ with respect to the calculated cross sections $\bar{\sigma}_{2k'}$ and $\bar{\sigma}_{3k'}$, where k' refers to the final best-fit potential (see below). As indicated by the χ^2_{2k} and χ^2_{3k} in Table II and by the nearly parallel $\bar{\sigma}_{1k}$ curves in Fig. 1(a), the energy dependence of the relative measurements is in agreement with that expected for three potential models from the literature. A selection of the true potential among these on the basis of the relative measurements is statistically insignificant. However, the large χ^2_{1k} values from Table II and the measured absolute $\hat{\sigma}_1$ in Fig. 1(a) with respect to the calculated $\bar{\sigma}_{1k}$ indicate that these potentials are not in agreement with our absolute data. For this reason a new set of parameters was determined in order to obtain a better fit of all the data.

The Born–Mayer-spline-dispersion potential from Eq. (3) was also used in this final fitting, mainly because it allows local changes in the interaction. We found that all measurements are mainly sensitive to the repulsive interaction, which could be completely specified by only three parameters, α, A, and A_0, for $R < R_0$, where R_0 is defined by $V(R_0) = 0$. The final best-fit potential is shown in Fig. 2, where it is compared with other experimental results[15,16] and results of recent *ab initio* calculations. One can estimate from the classical turning points of those partial waves, which make major contributions to the measured cross section at the highest energy, that the highest potential probed in the experiments was 220 meV. Since the experiments do not extend below 1400 m/sec they are not sensitive to details of the attractive-well region. We can, however, exclude the ϵ from Ref. 7 on the basis of all χ^2. The small ϵ of Ref. 6 also appears unlikely since it is difficult to find a physically meaningful potential form which would lead to agreement with our R_0 value. But fits combining the repulsive interaction either with the well from Ref. 5 (column 6, Table II) or with that of Ref. 6 (column 7, Table II) give practically identical results in the energy range under study, although the values of ϵ and C_6 differ by a factor of 2, approximately.

An indication on the true well depth could be the fact that calculations on the van der Waals constant C_6 from various authors[17,18] agree among each other and with the result of Ref. 5. For this reason we preferred the *ab initio* points of Ref. 5 in drawing the potential well in Fig. 2. But a statistically significant determination on the well is not possible at present on the basis of available measurements. This uncertainty allows a meaningful reduction of parameters in the potential model: Taking a most probable $C_6 = 2.83$ a.u., our $R_0 = 3.2$ Å, and a Lennard–Jones- (12, 6) potential form (a good approximation in the well region), ϵ is specified by $\epsilon = C_6 R_0^{-6}/4 = 0.39$ meV. In this way the following four-parameter potential is obtained:

$$V(R) = A(e^{-\alpha R} - e^{-\alpha R_0}) \quad \text{for } R < R_0$$
$$= 4\epsilon(x^{-12} - x^{-6}) \quad \text{with } x = R/R_0 \text{ for } R > R_0 . \tag{4}$$

This potential (last column, Table II) describes the beam experiments equally well and should be sufficient for practical purposes.

To determine ϵ and C_6 more accurately, measurements at lower velocities are required. We have performed full quantum-mechanical calculations of the H-He scattering extending down to energies of 4×10^{-7} eV (corresponding to a relative velocity $g = 10$ m/sec), keeping the repulsive part of the potential equal to that of the best-fit result (column 6, Table II). The whole negative region was multipled by factors between 0 and 2, given as parameters on the curves in Figs. 3 and 4, so that 0 corresponds to no attraction at all, 1 to the well from Ref. 5, and 2 approximately to the well from Ref. 6. Figure 3(a) shows the s- and p-wave phase shifts as function of relative velocity g and Fig. 3(b) shows the total cross section $\sigma(g)$, calculated from *all* phase shifts making nonvanishing

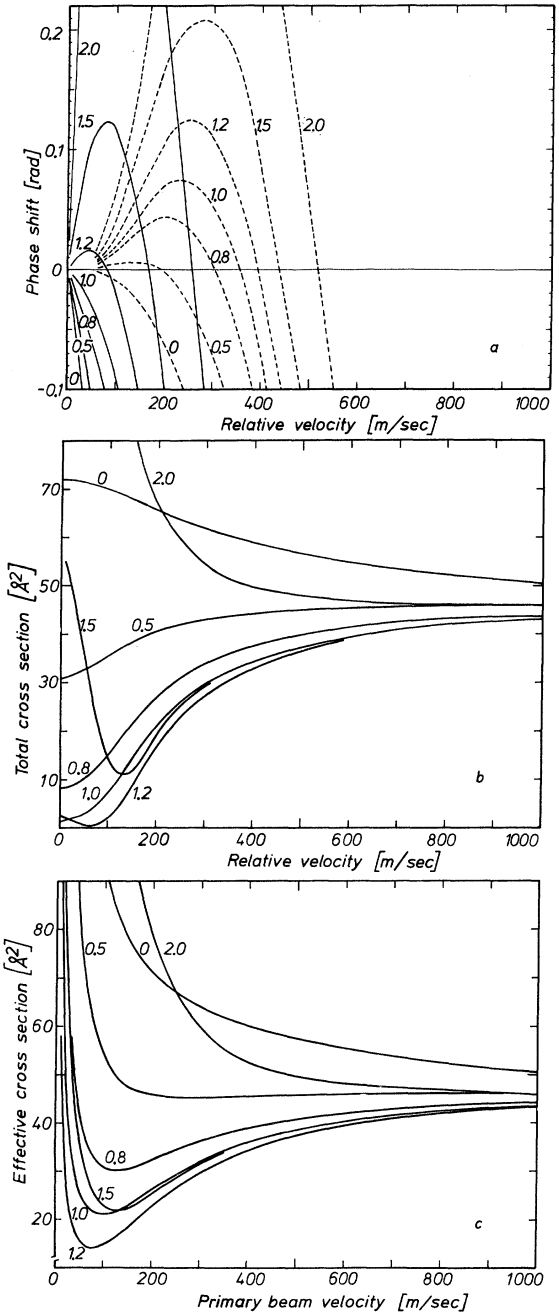

FIG. 3. (a) s-wave (solid line) and p-wave (dashed line) phase shifts as function of relative velocity for potential modifications explained in the text, for low-energy H-He scattering. (b) Total cross section $\sigma(g)$ as function of relative velocity g. (c) Effective cross section $\bar{\sigma}$ as function of primary beam velocity v, assuming 2 °K target temperature and 5% velocity resolution (FWHM).

partial cross sections $\sigma_l(g)$. The s-wave phase shifts η_0 [see Fig. 3(a)] approach zero at zero energy in every case. As a consequence of Levinson's theorem, for the H-He system and the potential variations under study, no bound states exist nor glory undulations in the total cross section. The latter are many-phase-shift phenomena, which require that in an η_l-vs-l plot (at fixed energy) the phase shifts become stationary at integer (glory-minimum) or half-integer (glory-maximum) multiples of π. In Fig. 3(b) the sharp minima in some total cross section curves at nonvanishing energies (corresponding to $g < 200$ m/sec) are due to the Ramsauer–Townsend effect,[19] a single-phase-shift phenomenon: The s-wave phase shift starts with positive gradient at zero energy and vanishes at a nonzero energy E_{RT}, where the other phase shifts ($l \geq 1$) are still so small that their partial cross sections σ_l make only minor contributions to σ.

We demonstrate this further in Fig. 4, where the nonvanishing σ_l and their sum σ are plotted against g in a logarithmic velocity scale ($10 < g < 500$ m/sec) for four potential wells (factors 1.0, 1.1, 1.2, and 1.3). Figure 4(b), corresponding to a factor of 1.1 (a 10% deeper well than that from Ref. 5), is especially interesting[20]: Even the s-wave contribution σ_0 remains negligible over a wide velocity range, making the He atom almost fully transparent for low-energy H atoms. This results from the fact that the *gradient* of the s-wave phase shift at zero energy, which determines the value of the cross section at zero energy, is nearly zero, due to a compensation of positive and negative potential regions.

From the $\sigma(g)$ in Fig. 3(b) we have calculated effective cross sections $\bar{\sigma}(v)$ as function of primary beam velocity, assuming a target-gas temperature of 2 °K and a primary-beam-velocity resolving power of 5%. As the curves in Fig. 3(c) clearly show, measurements at low velocities, which appear feasible in the near future, should

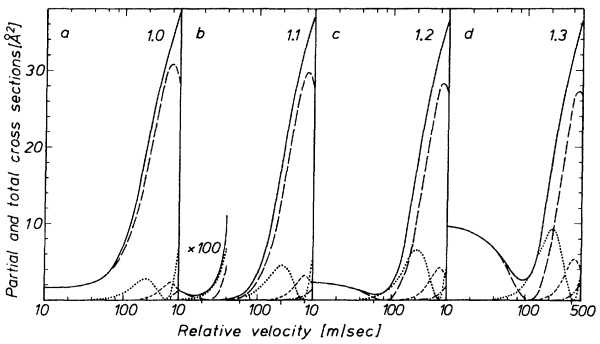

FIG. 4. Partial cross sections σ_0 (broken line), σ_1 (dotted line), σ_2 (dashed line), σ_3 (dash-dot), and resulting total cross section (solid line) for H-He as function of relative velocity g for four modifications of the potential well. Factors are (a) 1.0, (b) 1.1, (c) 1.2, and (d) 1.3.

make it possible to observe the Ramsauer–Townsend minimum in the H-He system and to determine ϵ with considerable accuracy.

We thank W. Schrader for help with the measurements and all members of the Bonn Molecular Beam Group for valuable discussions.

[1]E. A. Mason, J. Ross, and T. P. Schatz, J. Chem. Phys. 25, 626 (1956).
[2]C. R. Fisher and P. J. Kemney, J. Chem. Phys. 53, 50 (1970), and references therein.
[3]G. Das and S. Ray, Phys. Rev. Letters 24, 1391 (1970).
[4]W. H. Miller and H. F. Schaefer, J. Chem. Phys. 53, 1421 (1970).
[5]G. Das and A. C. Wahl, Phys. Rev. A 4, 825 (1971).
[6]W. D. Davison and Y. C. Liew, J. Phys. B 5, 309 (1972).
[7]B. Ulrich, A. L. Ford, and J. C. Browne, in *Abstracts of Papers of the Seventh International Conference on the Physics of Electronic and Atomic Collisions*, edited by L. M. Branscomb *et al.* (North-Holland, Amsterdam, 1971), pp. 208 and 209.
[8]The choice of D instead of H atoms has experimental reasons. The potentials of the isotopic systems are thought to be identical in the Born–Oppenheimer approximation. The different reduced masses are taken into account in our calculations of cross sections.
[9]R. Gengenbach, H. J. Strunck, and J. P. Toennies, J. Chem. Phys. 54, 1830 (1971); R. Gengenbach, Ph. D. thesis (Bonn, 1970) (unpublished).
[10]H. G. Bennewitz and W. Schrader (unpublished).
[11]W. C. Stwalley, A. Niehaus, and D. R. Herschbach, J. Chem. Phys. 51, 2287 (1969).
[12]R. W. Bickes, B. Lantzsch, J. P. Toennies, and K. Walaschewski (unpublished).
[13]R. Gengenbach, Ch. Hahn, and W. Welz (unpublished).
[14]J. W. M. DuMond and E. R. Cohen, Rev. Mod. Phys. 25, 691 (1953); CERN Report No. 64-13 (Geneva, 1964) (unpublished).
[15]I. Amdur and E. A. Mason, J. Chem. Phys. 25, 630 (1956).
[16]Yu. N. Belyaev and V. B. Leonas, Dokl. Akad. Nauk SSSR 173, 306 (1967) [Sov. Phys. Doklady 12, 233 (1967)].
[17]P. M. Getzin and M. Karplus, J. Chem. Phys. 53, 2100 (1970).
[18]D. A. McQuarrie, J. Tereby, and S. J. Shire, J. Chem. Phys. 51, 4683 (1969), and references therein.
[19]See, e.g., S. Geltman, *Topics in Atomic Scattering Theory* (Academic, New York, 1969), pp. 23–26.
[20]A similar result with a Lennard–Jones potential was obtained by H. G. Bennewitz and H. D. Dohmann (unpublished).

PHYSICAL REVIEW A VOLUME 7, NUMBER 1 JANUARY 1973

Total Inelastic Cross Section for Collisions of H_2 with Fast Charged Particles*

J. W. Liu
Department of Chemistry, Indiana University, Bloomington, Indiana 47401
(Received 14 April 1972; revised manuscript received 20 September 1972)

A sum rule due to Inokuti *et al.* for the Bethe inelastic cross section for fast-charged-particle collisions with atoms and molecules has been applied to H_2. Using an accurate two-center configuration-interaction wave function, the formula for nonrelativistic incident particles was found to be given as $\sigma_{tot}=4\pi a_0^2 z^2 (R/T)[1.5487 \ln(T/R)+2.2212]$ to within an error of 0.5% in σ_{tot} for incident-electron energies above 1 keV. Although the theoretical values are in good agreement with the summed experimental (i) total ionization (including dissociation ionization), (ii) total dissociative excitation, and (iii) most important discrete excitation cross sections, an apparent systematic trend suggests that one or more of the current experimental total cross sections for electron impact on H_2 may not be accurate and that omitted processes should be included for comparison in the incident energy range above 1 keV.

I. INTRODUCTION

A very accurate evaluation of the total inelastic cross section for high-incident-energy charged-particle collisions has been reported[1] for He, Li^+, and H^-. For the H_2 molecule, the theoretical evaluation of this inelastic cross section has not been reported because of the greater difficulties encountered in the evaluation of the optical quantity $L(-1)$, the oscillator-strength moment $S(-1)$, and the quantities I_1 and I_2 which were defined previously by Inokuti and Kim *et al.*[1] (see Sec. II). Recently the total inelastic differential cross sections[2] in the first Born approximation have been reported using five-term configuration interaction (CI)[3] and ten term CI[4] wave functions containing 95 and 97% of the binding energies, respectively. The quantity I_1 can be obtained from the calculated total inelastic differential cross sections. An estimate of the optical quantity $L(-1)$ has also recently been reported by Langhoff and Yates.[5] In addition, the quantity I_2 can be calculated by using the CI wave functions previously used for calculating I_1. Using these, a sum rule for the Bethe cross sections can be obtained with less than 1% uncertainty in the high-energy limit according to the method of Inokuti *et al.*[1] The experimental study of the impact phenomena of H_2 by fast charged